

# Optimization of preparation and property studies on glycosylated albumin as drug carrier for nanoparticles

YUAN GAO<sup>1</sup>, WANJIN SUN<sup>1,3</sup>, JIANJUN ZHANG<sup>2,3</sup>*Received November 16, 2010, accepted January 10, 2011**Sun Wanjin, School of Traditional Chinese Medicine, China Pharmaceutical University, 210009 Nanjing, P.R. China  
amicute@163.com**Pharmazie 66: 484–490 (2011)**doi: 10.1691/ph.2011.0850*

Glycosylated BSA was prepared via Maillard reaction and central composite design (CCD) technique was applied to study the effects of reaction time, temperature, the pH value of the buffer solution on the degree of graft (DG), content of the melanoid (A420) and emulsifying stability (ES) of the resultant product. Fluorescence spectra as well as several other techniques including sodium dodecyl sulfate polyacrylamide gel electrophoresis (SDS-PAGE), infrared spectrum (IR) and differential scanning calorimetry (DSC) were employed to study the possible differences between the glycosylated BSA and BSA. Glycosylated albumin possessed distinct properties from BSA and had the great potential to be used as the drug carrier for nanoparticles.

## 1. Introduction

Albumin plays more and more important roles as the drug carriers in clinical use for its ability of improving both physical and pharmacokinetic properties of drugs. American Bioscience Inc. has developed a unique albumin-based nanoparticles technology (nab<sup>®</sup> technology) which is ideal for encapsulating lipophilic drugs into nanoparticles. This technology makes paclitaxel albumin nanoparticles a dramatic antitumor drug with market approval known as Abraxane<sup>™</sup>. Following its approval in January 2005, Abraxane is being further evaluated and improved (Ibrahim et al. 2002). In order to enhance the targeting property of Abraxane, we tried to couple albumin with some suitable tumor related receptors. As an integrin receptor, CR3 is overexpressed by the tumor endothelium and can recognize polysaccharide groups including dextran (Bishop and Gagneux 2007; Guan and Mariuzza 2007; Cobb and Kasper 2005), so a glycosylated albumin which has the ability to target tumor endothelium is the very drug carrier we found for anticancer drugs. Hitherto, different proteins such as ovalbumin, lysozyme and bovine serum albumin (BSA) have been conjugated with polysaccharides, mainly dextran, chitosan or galactomannan, with the aim to improve their solubility, emulsifying properties and heat stability (Oliver et al. 2006).

An effective method to produce the glycosylated albumin, which does not require chemical catalysis, just relies on the interaction of albumin with polysaccharides via Maillard reaction. The early stage of Maillard reaction involves a condensation between the carbonyl group of a reducing carbohydrate with an available, unprotonated amino group, mainly the  $\epsilon$ -amino group of the Lys residues in albumin. With aldoses, such as glucose, this leads to a Schiff base with the release of water. The Schiff base subsequently cyclises to the corresponding N-glycosylamine, which then undergoes an irreversible Amadori rearrangement to produce the Amadori compound. The intermediate stage begins with the degradation of the Amadori product following various divergent pathways to give a large multiplicity of poorly

characterized compounds. In the final stage, highly colored, insoluble, nitrogen-containing polymeric compounds, referred to as melanoid, are formed. Ideally, to produce a drug carrier for nanoparticles used by patients, Maillard reaction needs to be performed under carefully controlled conditions to prevent the later two stage changes (Kato 2002). The degree of free amino groups (FAG) change (Spellman et al. 2003) in albumin were introduced to represent the efficiency of Maillard reaction in this study, and based on a Lambert-Beer principal, the content of melanoid which urgently needs to be monitored (Papanastasiou et al. 1994), was evaluated by the absorbance at 420 nm. Central composite design (CCD) technique is commonly used for processing analysis and modeling which is more effective than the factorial design. CCD can give almost as much information as a multilevel factorial, but requires much fewer experiments than a full factorial. In the present study, CCD technique was applied to study the effects of reaction time, temperature, the pH value of the buffer solution on the resultant product so as to optimize the preparation of glycosylated BSA via Maillard reaction. Then the glycosylated BSA was characterized by fluorescence spectra, SDS-PAGE, IR and DSC to acquire more information about it.

## 2. Investigations, results and discussion

Preliminary experiments were performed to select the levels of constraints of the crucial factors in Maillard reaction. It was demonstrated that the reaction time should be limited to 12–36 h; the temperature needed to be controlled between 55 and 65 °C and pH value would be better at the range of 7.5–9.5. The optimum reaction procedure is selected to have a resultant product with DG (%) as high as possible, A(420) as low as possible and ES as large as possible. The CCD including the factors, responses and the results from each test are listed in Table 1. Factors influencing DG (%) and how they affect are shown in Table 2. The results showed that pH value provided the

**Table 1: Experimental design and the results**

Std	Run	Type	Time (h)	Temp (°C)	pH	DG (%)	A(420)	ES
9	2	Center	24	60	8.5	25.16	0.009	178.0
11	4	Center	24	60	8.5	29.09	0.007	179.5
10	9	Center	24	60	8.5	25.47	0.006	191.1
12	11	Center	24	60	8.5	28.21	0.011	168.4
20	13	Center	24	60	8.5	28.43	0.010	158.0
19	17	Center	24	60	8.5	30.29	0.010	172.8
16	14	Axial	24	65	8.5	17.23	0.014	102.0
13	15	Axial	12	60	8.5	22.28	0.004	146.7
17	16	Axial	24	60	7.5	6.81	0.005	186.6
15	18	Axial	24	55	8.5	31.51	0.007	171.3
18	19	Axial	24	60	9.5	40.93	0.008	89.5
14	20	Axial	36	60	8.5	39.83	0.017	182.9
6	1	Fact	31	57	9.1	34.32	0.013	111.5
5	3	Fact	17	57	9.1	21.74	0.008	126.3
7	5	Fact	17	63	9.1	19.43	0.010	118.2
3	6	Fact	17	63	7.9	6.62	0.003	146.7
4	7	Fact	31	63	7.9	18.90	0.016	172.0
8	8	Fact	31	63	9.1	29.95	0.017	131.5
1	10	Fact	17	57	7.9	14.90	0.002	144.3
2	12	Fact	31	57	7.9	20.20	0.010	156.2

largest contribution to DG (%) and ES, wherever the temperature had more limited effects on them. All three factors somewhat affected A(420), among them the reaction time played a more important role. The responses were individually fitted to models including Linear, 2FI, Quadratic and Cubic. Each obtained model was validated by P value and R<sup>2</sup>. The design expert software will suggest the fitting model automatically. The resultant equations for the responses are given below:

$$\begin{aligned} \text{DG (\%)} = & 28.56 + 5.14A - 2.95B + 7.48C \\ & + 0.62AB + 0.69AC + 0.36BC - 0.094A^2 \\ & - 2.46B^2 - 2.63C^2 \quad (R^2 = 0.9242, \text{SD}=3.60) \end{aligned} \quad (1)$$

$$\begin{aligned} \text{A(420)} = & 9.354 \times 10^{-3} + 4.017 \times 10^{-3}A \\ & + 1.814 \times 10^{-3}B + 1.614 \times 10^{-3}C \\ & (R^2 = 0.8165, \text{SD} = 2.163 \times 10^{-3}) \end{aligned} \quad (2)$$

$$\begin{aligned} \text{ES} = & 174.92 + 7.07A - 6.33B - 21.60C \\ & + 5.19AB - 4.84AC - 0.79BC - 4.85A^2 \\ & - 14.80B^2 - 14.31 C^2 \quad (R^2 = 0.8807, \text{SD} = 19.41) \end{aligned} \quad (3)$$

**Table 2: Factors influencing the responses**

Response	Factor	Correlation
DG (%)	Time	0.470
	Temperature	-0.270
	pH	0.685
A(420)	Time	0.773
	Temperature	0.349
	pH	0.311
ES	Time	0.200
	Temperature	-0.179
	pH	-0.612

where A is the time of Maillard reaction, B is the temperature and C is the pH value of the buffer solution.

It can be seen from the corresponding coefficient before every highest term in each equation, that DG (%) was obviously affected by the reaction time and pH value but just mildly affected by the temperature. The tendency seems to be the same with ES. As to A(420),  $4.017 \times 10^{-3}$  is the largest coefficient in the highest term, so the reaction time may provide the largest contribution to A(420).

Based on the binomial fitting equations of all the indicators, three-dimensional response surfaces are generated and shown in Fig. 1. In this study, three variables which makes the least contribution will be fixed and set as the center value and the other two will be the corresponding indexes, after substituting into the objective function equation, predicted 3D response surface of Maillard reaction are generated.

The optimized conditions and the bias between the predicted and the observed parameter are presented in Table 3, values agreed well. Due to the small cardinal value of A(420), the bias (%) seems a large value but actually it reaches a relatively precise extent. CCD was efficiently applied to optimize the production of glycosylated BSA. The optimized conditions for reaction were: Dissolving BSA and dextran in pH 8.5 Tris-HCl buffer solution with molar ratio of 1:3, lyophilizing, keeping the protein-carbohydrate mixtures under vacuum in desiccators equilibrated at 58 °C RH 79% for 20 h.

The particle size of glycosylated BSA was determined to be 100.5 nm with a polydispersity index (PI) of 0.365. BSA underwent the same Maillard reaction procedure as glycosylated BSA was determined to be 120.2 nm with a PI of 0.461, and the physical mixture of BSA and dextran was determined to be 110.2 nm with a PI of 0.308. It can be concluded that the existence of dextran exhibited more stable feathers than BSA, probably due to the stereo effect of polysaccharide.

Fluorescence spectroscopy was used to find the possible difference between the glycosylated BSA and BSA. The emission fluorescence spectra of glycosylated BSA and BSA as well as the mixture of BSA and dextran are shown in Fig. 2. Red shift or blue shift in the spectroscopy indicates the structural changes of albumin (Carter and Ho 1994). The tryptophans occupy the 134 and 212 position in the BSA polypeptide chain, and in the tertiary

**Table 3: Optimized conditions and their validation**

	Time(h)	Temp(°C)	pH	DG (%)	A(420)	ES
Predicted	19.94	57.87	8.47	26.40	0.006	169.1
Actual	20	58	8.5	25.83 ± 1.10	0.005 ± 0.001	175.0 ± 5.4
Bias (%)				2.2	12.5	3.4

structure of BSA they are located in subdomains IB and IIA. The 20 tyrosine residues are mainly located in subdomains IB, IIA and IIIA of BSA structure. The above mentioned amino acids provide the largest contribution to fluorescence absorption and are sensitive to structure changes (Sulkowska 2002; Steiner and Weinryb 1971). Glycosylated BSA showed a red shift from BSA, which suggested a tertiary structure change of BSA. However, no significant shift between the physical BSA/dextran mixture and BSA can be found, so the tertiary structure of BSA will change only through Maillard reaction.

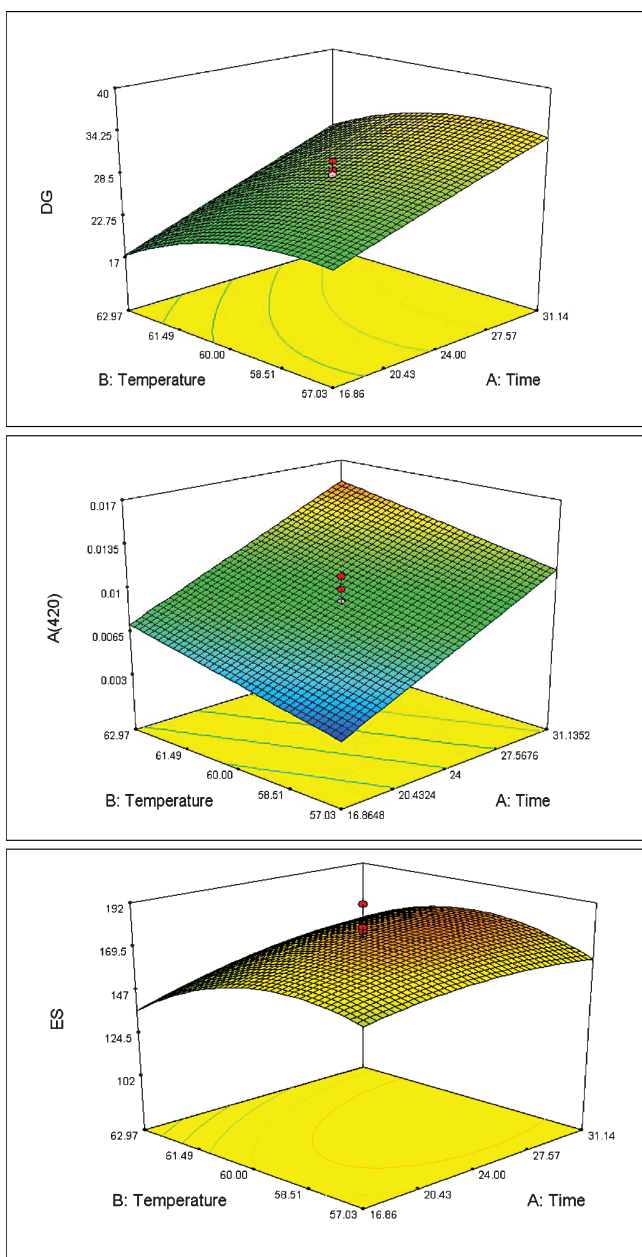


Fig. 1: Predicted 3D response surface of Maillard reaction

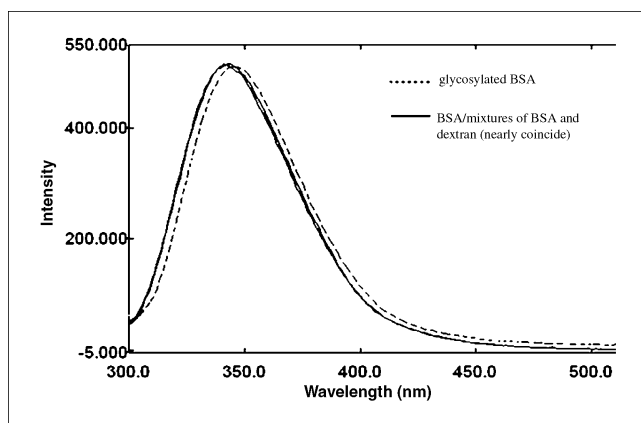
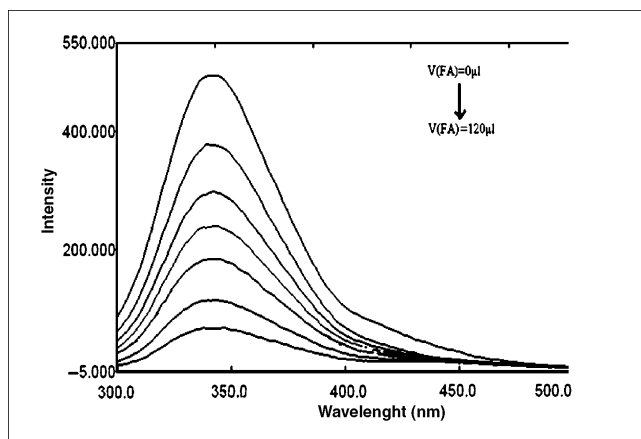
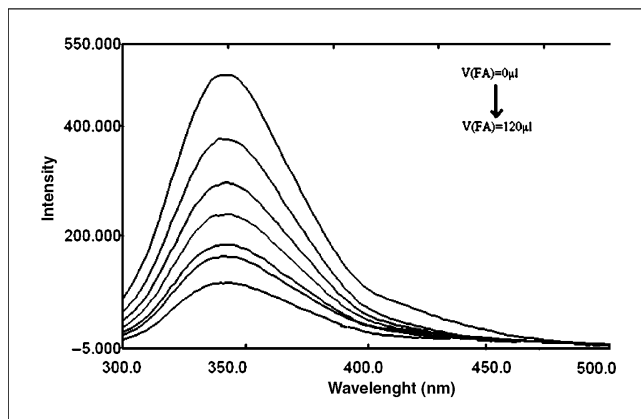


Fig. 2: Fluorescence spectra of glycosylated BSA, BSA and mixtures of BSA and dextran

FA (1.1 mg/mL) with a volume interval of 20 µl was added into glycosylated BSA solutions or BSA solution both at a concentration of 0.66 mg/mL. The effect of FA on the two protein solutions was shown in Fig. 3. The relative fluorescence intensity of glycosylated BSA and BSA decreased with addition amount of FA.



(A)



(B)

Fig. 3: Effect of FA on fluorescence spectra of (A) glycosylated BSA and (B) BSA

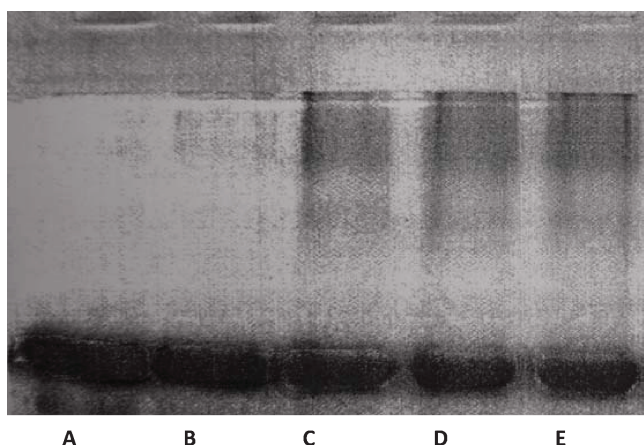


Fig. 4: SDS-PAGE analysis of BSA (lane A), physical mixture of BSA and dextran (lane B), glycosylated BSA (lane C-E)

To analyze the interaction between them, Stern–Volmer equation (4) and Scatchard equation (5) were introduced.

$$\frac{F_0}{F} = 1 + K_q \tau_0 [D] = 1 + K_{sv} [D] \quad (4)$$

$F_0$  and  $F$  are the relative fluorescence of protein in the absence and presence of quencher  $[D]$ , respectively.  $K_{sv}$  is the quenching constant, and  $[D]$  is the quencher concentration.

$$\log \left[ \frac{F_0 - F}{F} \right] = \log K_b + n \log [D] \quad (5)$$

$K_b$  is the binding constant for the ligand–albumin complex and  $n$  refers to the number of binding sites in albumin.

All constants are listed in Table 4. The regression coefficient showed that Scatchard equation was more suitable for these systems and the binding force between glycosylated BSA and FA was stronger than it between BSA and FA. The number of binding sites can indicate even slight changes of the protein structure. As shown in Table 4, binding sites increase remarkably in glycosylated BSA probably due to the exposition of the hydrophobic residue by heating in Maillard reaction. This was a positive and beneficial result, because the increase of hydrophobic area will potentially increase the drug loading of glycosylated BSA as drug carrier.

SDS-PAGE analysis demonstrated that the molecular mass of glycosylated BSA was higher than BSA after binding with dextran (Fig. 4). The physical mixture of BSA and dextran was also investigated as a reference (Fig. 4B) and a similar SDS-PAGE profile was observed. BSA underwent the same Maillard reaction indicating that the substance with higher molecular mass was not a BSA aggregate due to heating.

The infrared spectra of glycosylated BSA, dextran, BSA as well as the mixture of BSA and dextran are shown in Fig. 5. The infrared portion of the electromagnetic spectrum is usually divided into three regions; the near-, mid- and far- infrared, named for their relation to the visible spectrum. The higher energy near-IR, approximately  $14000\text{--}4000\text{ cm}^{-1}$  can excite overtone or harmonic vibrations. The mid-infrared, approximately  $4000\text{--}400\text{ cm}^{-1}$  can be used to study the fundamental vibrations and associated rotational vibrational structure. The far-infrared, approximately  $400\text{--}10\text{ cm}^{-1}$ , lying adjacent to the microwave region, has low energy and may be used for rotational spectroscopy. The names and classifications of these subregions are conventions, and are only loosely based on the relative molecular or electromagnetic properties. As shown in Fig. 5A,  $3200\text{--}3500\text{ cm}^{-1}$  was relevant to stretching vibration of N-H and  $3100\text{--}2500\text{ cm}^{-1}$ , indicating the characteristic absorption band

of BSA (Xiao et al. 2007; Zhou et al. 2007).  $1680\text{--}1630\text{ cm}^{-1}$  showed the existence of the amide and  $1600\text{--}1500\text{ cm}^{-1}$  contained a stretching vibration of C-N and bending vibration of N-H.  $3380, 2924, 1650, 1016$  and  $1157\text{ cm}^{-1}$  in Fig. 5B may be relevant to stretching vibration of OH, stretching vibration of C-H, carbonyl group, stretching vibration of CO (C-O-C, C-OH) respectively. Fig. 5C represents the physical mixture of BSA and dextran with the molecular ratio of 1:3. Due to the large proportion of dextran, the spectrum displayed nearly the features of dextran. After Maillard reaction, as shown in Fig. 5D, the characteristic absorption band of BSA significantly diminished, indicating the participation of amino acid in reaction.  $1650\text{ cm}^{-1}$  carbonyl group in chain structure of dextran disappeared,  $1640\text{ cm}^{-1}$  can be identified as amides from remaining BSA. The carbonyl group was involved in Maillard reaction generating the glycosylated BSA.

The thermograms of BSA, dextran, the physical mixture of BSA and dextran as well as the glycosylated BSA are presented in Fig. 6. A melting endotherm was obtained with BSA at  $214.3\text{ }^\circ\text{C}$  (Fig. 6A), and two were obtained with dextran at  $242.9\text{ }^\circ\text{C}$  and  $265.4\text{ }^\circ\text{C}$  (Fig. 6B). The mixture of BSA and dextran showed two melting endotherm without much change in peak shape or position (Fig. 6C). The DSC thermogram of the glycosylated BSA showed a melting exotherm at  $170.7\text{ }^\circ\text{C}$  (Fig. 6D), demonstrating the existence of a new compound different from BSA and dextran.

## 3. Experimental

### 3.1. Materials

BSA and dextran with average molecular weight of 20 kDa were purchased from Sigma Chemical Inc. (St. Louis, MO, USA). 5% (W/V) Trinitrobenzenesulphonic acid (TNBS) solution was purchased from Aladdin Chemical Ltd. (Shanghai, China). Other chemicals were at least of analytical grade.

### 3.2. Preparation of glycosylated BSA

In our preliminary study, serials of monofactorial investigations had been carried out to select the proper preparing method, types of buffer salt, the pH value of the buffer solution and temperature, humidity, reaction time for Maillard reaction. The degree of graft (DG), content of the melanoid ( $A_{420}$ ) and emulsifying stability (ES) of each obtained product was examined, and results reflected that the resultant products can be mainly affected by many factors, of which the temperature, reaction time, pH value of the buffer solution provided the largest contribution to all the properties of the resultant product. However, monofactorial investigation had limited ability to make sure the precise value for those crucial factors.

In statistics, a CCD is an experimental design, useful in response surface methodology, for building a second order model for the response variable without needing to use a complete three-level factorial experiment. After the designed experiment is performed, linear regression is used, sometimes iteratively, to obtain results. Coded variables are often used when constructing this design. CCD technique was applied to further optimize the preparing conditions. The general preparing method was as follows: Albumin and polysaccharide were dissolved in Tris-HCl buffer solution of a certain pH value in the molar ratio of 1:3 and lyophilized. The protein–carbohydrate mixtures were then kept under vacuum in desiccators equilibrated at a certain temperature and RH 79% for a period of time. After incubation, the products were reconstituted in distilled water to a protein concentration of  $6.6\text{ mg/mL}$ . All experiments were carried out in duplicate.

### 3.3. Degree of graft (DG)

The number of free amino groups (FAG) was measured using TNBS method (Satake et al. 1960) by a 1500 Multiskan spectrum microplate reader (Thermo Electron Inc., USA). TNBS was diluted using  $\text{NaHCO}_3$  solution (4%, pH 8.5) to be  $4\text{ }\mu\text{mol/mL}$ .  $65, 135, 205, 270, 340, 480\text{ }\mu\text{L}$  of the solution were precisely transferred to a 5 mL volumetric flask, and each was taken in double. In one flask,  $0.1\text{ mL}$  of 1% trichloroacetic acid and  $0.1\text{ mL}$  of L-valine ( $40\text{ }\mu\text{mol/mL}$ ) were added. In another one, only  $0.1\text{ mL}$  of 1% trichloroacetic acid was added as the reference. Both flasks were then kept in dark to react for 1 h at  $40\text{ }^\circ\text{C}$  and the reaction was terminated by adding  $0.5\text{ }\mu\text{mol/mL}$  HCl solution to the volume. The absorbance (A) was mea-

**Table 4: Number of binding sites of folic acid with glycosylated BSA and BSA**

FA	Stern-Volmer model			Scatchard model		
	R <sup>2</sup>	Ksv(L/mol)	Kq(L/mol·s)	R <sup>2</sup>	lgK <sub>b</sub>	n
Glycosylated BSA	0.9397	30291	3.0291 × 10 <sup>12</sup>	0.9923	25.813	2.2725
BSA	0.9498	24686	2.4686 × 10 <sup>12</sup>	0.9942	18.355	1.6217

sured at 410 nm. The relationship between TNBS concentration (C) and A was:  $A = 0.0225 + 1.7199C$ ,  $R = 0.9986$ .

0.5 mL of the reconstituted solution resulted from Maillard reaction was added into 4 mL of TNBS solution (4 μmol/mL) and was kept in dark to react for 1 h at 40 °C. The complex solution was isolated by centrifugation (1000 rpm for 10 min). 0.9 mL of the supernatant was transferred into two volumetric flasks (5 mL), respectively. In one flask, 0.1 mL of 1% trichloroacetic acid and 0.1 mL of L-valine (40 μmol/mL) were added. In another one, only 0.1 mL of 1% trichloroacetic acid was added as the reference. Both flasks were then kept in dark to react for 1 h at 40 °C and the reaction was terminated by adding 0.5 μmol/mL HCl solution to the volume. The values of absorbance measured at 410 nm were transformed into μmoles of FAG/mL using the calibration curve.

DG was introduced to demonstrate the degree of FAG change in Maillard reaction and was calculated by the following equation:

$$DG (\%) = \frac{(C_0 - C_t)}{C_0} \times 100\% \quad (6)$$

where  $C_t$  (μmol/g) is the concentration of FAG in glycosylated BSA at time  $t$ ,  $C_0$  (μmol/g) is the concentration of FAG in albumin without dextran at the same condition. As this regard, DG (%) can represent the efficiency of reaction free of environmental interference.

### 3.4. Melanoidins content ( $A_{420}$ )

The brown color development was evaluated by the absorbance at 420 nm ( $A_{420}$ ) measured (TU1800 UV spectrophotometer, Puxi General Instruments Ltd., Beijing, China). The samples were centrifuged at 10000 rpm for 10 min to reduce the scattering effect due to protein aggregates (Laura et al. 2007; Brands and van Boekel 2003).

### 3.5. Emulsifying stability (ES)

In our study, glycosylated BSA was developed as the potential carrier. It may undergo high pressure homogenization in the formulation process. So the emulsifying stability (ES) was investigated to ensure the quality of the intermediate product.

ES was determined by the turbid metric method (Pearce and Kinsella 1978). 2 mL soybean oil was added into 4 mL of the complex solution and homogenized (FA25 mechanical homogenizer, Anpu Instruments Ltd., Shanghai, China) at 10000 rpm for 1 min to produce the emulsion. Then 50 μL of emulsion were pipetted at 0 and 10 min after homogenization and mixed with 5 mL of 0.1% sodium dodecyl sulfate (SDS). Absorbance of the emulsion was measured at 500 nm and the emulsion stability index was computed

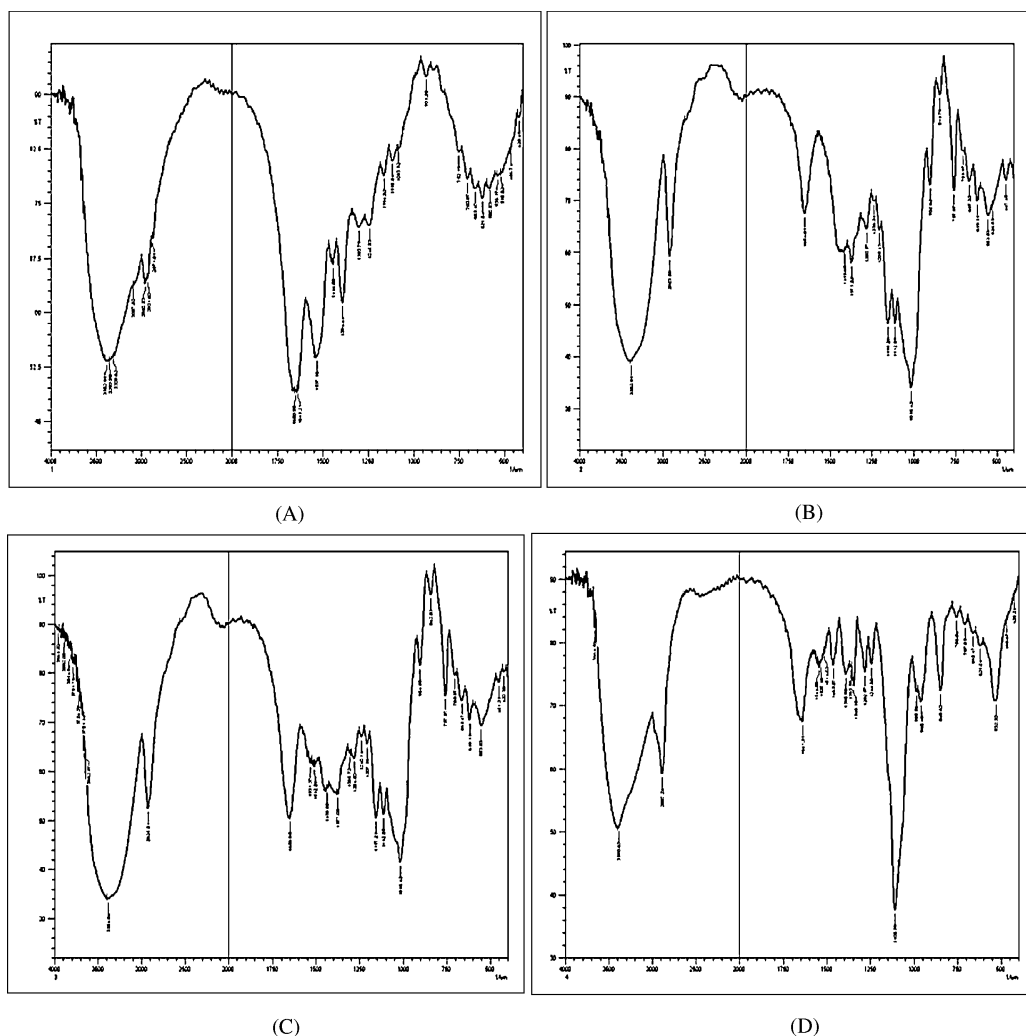


Fig. 5: Infrared Spectrum of (A)BSA; (B) dextran; (C) mixtures of BSA and dextran; (D) glycosylated BSA

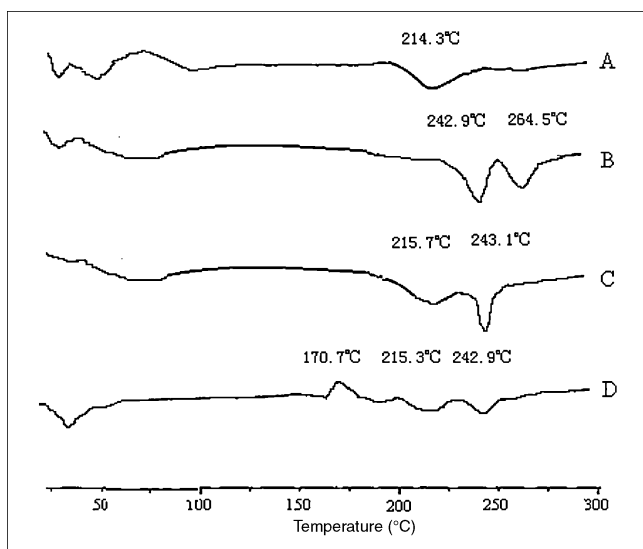


Fig. 6: DSC thermograms of (A) BSA; (B) dextran; (C) the physical mixture of BSA and dextran; (D) glycosylated BSA

according to the following equation:

$$ES = \frac{A_0}{A_0 - A_t} \times T \quad (7)$$

where T is the time interval (10 min in this study).

### 3.6. Particle size analysis

The particle size analysis was performed by photon correlation spectroscopy (PCS) using a Zetasizer 3000 (Malvern Instruments, Malvern, UK). Prior to measurement, the products were reconstituted in distilled water to a proper concentration and dispersed homogeneously. Mean particle size and the polydispersity index (PI) of the glycosylated BSA, BSA which underwent the same Maillard reaction without the existence of dextran, as well as the physical mixture of BSA and dextran were recorded.

### 3.7. Fluorescence spectra

In our early study, the interaction of folic acid (FA) with BSA had been investigated in detail. FA could quench the inner fluorescence of BSA by forming the FA-BSA complex. Both static quenching and non-radiative energy transferring were confirmed to result in the fluorescence quenching. The interaction between them seems to be strong and the binding force was mainly hydrophobic force (Shu et al. 2010). Based on this result, Fluorescence quenching method was employed to study the possible difference between the glycosylated BSA and BSA in order to compare their hydrophobic area and to deduce the spatial structure change in glycosylated BSA.

Emission fluorescence spectra of glycosylated BSA and BSA as well as the mixture of BSA and dextran at the same protein concentration (0.66 mg/mL) with a wavelength range of 300–500 nm on the spectrofluorimeter (Shimadzu RF-5301, Japan) were recorded at an excitation wavelength of 280 nm. The binding of FA to glycosylated BSA was studied by monitoring the changes in the emission fluorescence spectra of protein in the presence of FA at 280 nm. The binding of FA to BSA at the same concentration was employed as the reference group.

### 3.8. Sodium dodecyl sulfate polyacrylamide gel electrophoresis (SDS-PAGE)

SDS-PAGE is a technique widely used in biochemistry, forensics, genetics and molecular biology to separate proteins according to their electrophoretic mobility. The composition of resolving gel (10%) and stacking gel (5%) is listed in Table 5. A Tanon EPS 300 electrophoresis apparatus (Tianneng Science Co., Ltd, Shanghai, China) was set up with cathode buffer covering the gel in the negative electrode chamber, and anode buffer in the lower positive electrode chamber. The denatured sample proteins were added to the wells one end of the gel with a syringe or pipette. Finally, the apparatus was hooked up to a power source under appropriate running conditions to separate the protein bands. BSA which underwent the same Maillard reaction without the existence of dextran and the physical mixture of BSA and dextran were employed as reference group.

Table 5: Composition of resolving gel (10%) and stacking gel (5%)

Component	Resolving gel	Stacking gel
	V (ml)	V (ml)
Distilled water	4.0	3.40
Solution of acrylamide (30%)	2.5	0.83
1.5 M Tris HCl (pH 8.8)	2.5	/
1.0 M Tris HCl (pH 6.8)	/	0.63
Solution of SDS (10%)	0.10	0.05
Solution of ammonium persulfate (10%)	0.10	0.05
TEMED	0.004	0.005

### 3.9. Infrared spectrum (IR)

A Thermo Nicolet Impact 410 FTIR Spectrophotometer (Thermo Fisher Scientific Inc., USA) with a spectral resolution of  $1 \text{ cm}^{-1}$  was used in KBr diffuse reflectance mode for collecting the FTIR spectra of the solid glycosylated BSA, dextran, BSA as well as the physical mixture of BSA and dextran. 64 scans were collected over the range of  $4000\text{--}400 \text{ cm}^{-1}$ . Data were analyzed using Nicolet Omnic software (version 8.0).

### 3.10. Differential scanning calorimetry (DSC)

The thermal analyses were performed using a differential scanning calorimeter (NETZSCH DSC 204, Germany) to determine possible difference among the glycosylated BSA, dextran, BSA as well as the physical mixture of BSA and dextran. The DSC runs were performed over a temperature range of 30 to  $300 \text{ }^\circ\text{C}$  at a heating rate of  $10 \text{ }^\circ\text{C}$  per minute in an open pan using alumina as a reference material. Data analysis was performed using NETZSCH-Proteus software (version 4.2).

### 3.11. Experimental design and data analysis

It is assumed in the central composite design that the central point for each factor is 0, and the design is symmetric around this (Brereton 2003). For three variables ( $n=3$ ), the central composite design can be represented by points on a cube, each axis corresponding to a factor and consists of 20 experiments, including  $2^n$  ( $2^3=8$ ) factor points,  $2^n$  ( $2 \times 3=6$ ) axial points and 6 center points (six replications). The 20 experiments comprised in the central composite design were performed in two blocks. A design expert software package Design-Expert (version 7.0, Stat-Ease, Inc.) was used to generate the design. The factorial design points were executed in one block in random order and then the axial experiments done in another randomized block. The factors in this experiment were the time of Maillard reaction (A), reaction temperature (B) as well as pH value of the buffer solution (C) and the responses were DG (%), A(420), ES of the resultant product from Maillard reaction.

Acknowledgments: This work was funded by The Technology Platform for New Formulation and New DDS, Important National Science & Technology Specific Projects, NO:2009ZX09310-004, Peak of six major talents in Jiangsu Province (Level A) and Natural Science Projects of Jiangsu Province, NO:SBK20080571.

### References

- Bishop JR, Gagneux P (2007) Evolution of carbohydrate antigens-microbial forces haping host glycomes. *Glycobiology* 17: 23R-34R.
- Brands CMJ, van Boekel MAJS (2003) Kinetic modelling of reactions in heated disaccharide casein Systems. *Martinus Food Chem* 83: 13–26.
- Brereton RG (2003) *Chemometrics: Data Analysis for the Laboratory and Chemical Plant*. John Wiley, 76–84.
- Carter DC, Ho JX (1994) Structure of serum albumin. *Adv Protein Chem* 45:153–203.
- Cobb BA, Kasper DL (2005) Coming of age: carbohydrates and immunity. *Eur J Immunol* 35: 352–356.
- Guan RR, Mariuzza A (2007) Peptidoglycan recognition proteins of the innate immune system. *Trends Microbiol* 15: 127–134.
- Ibrahim NK, Desai N, Legha S, Soon-Shiong P, Theriault RL, Rivera E, Esmaeli B, Ring SE, Bedikian A, Hortobagyi GN, Ellerhorst JA (2002) Phase I and pharmacokinetic study of ABI-007, a cremophor free, protein-stabilized, nanoparticle formulation of paclitaxel. *Clin Cancer Res* 8: 1038–1044.

- Jiménez-Castaño L, Villamiela M, López-Fandiño R (2007) Glycosylation of individual whey proteins by Maillard reaction using dextran of different molecular mass. *Food Hydrocolloids* 21: 433–443.
- Kato A (2002) Industrial applications of Maillard-type protein-polysaccharide conjugates. *Food Sci Tech Res* 8: 193–199.
- Oliver CM, Melton LD, Stanley RA (2006) Creating proteins with novel functionality via the Maillard reaction: A review. *Crit Rev Food Sci Nutr* 46: 337–350.
- Papanastasiou P, Grass L, Rodela H, Patrikarea A, Oreopoulos D, Diamandis EP (1994) Immunological quantification of AGEs in serum of patients on haemodialysis or peritoneal dialysis. *Kidney Int* 46: 216–222.
- Pearce KN, Kinsella JE (1978) Emulsifying properties of proteins: evaluation of a turbidimetric technique. *J Agric Food Chem* 26: 716–718.
- Satake K, Okuyama T, Ohashi M, Shinoda T (1960) The spectrophotometric determination of amine, amino acid and peptide with 2,4,6-trinitrobenzene 1-sulfonic acid. *J Biochem* 47: 654–660.
- Shu WJ, Sun WJ, Gao Y, Zhang JJ (2010) Interaction of folic acid and deoxycholic acid with bovine serum albumin as well as the effects of coexisting paclitaxel. *J Chin Pharm Uni* 41: 253–258.
- Spellmana D, McEvoya E, O’Cuinnb G, FitzGerald RJ (2003) Proteinase and exopeptidase hydrolysis of whey protein: Comparison of the TNBS, OPA and pH stat methods for quantification of degree of hydrolysis. *Int Dairy J* 13: 447–453.
- Steiner RF, Weinryb I (1971) Excited states of proteins and nucleic acids. Plenum Press (New York) 396–473.
- Sulkowska A (2002) Interaction of drugs with bovine and human serum albumin. *J Mol Struct* 614: 227–232.
- Xiao J, Shi J, Cao H, Wu S, Ren F, Xu M (2007) Analysis of binding interaction between puerarin and bovine serum albumin by multi-spectroscopic method. *J Pharm Biomed Anal* 45: 609–615.
- Zhou B, Qi ZD, Xiao Q, Dong JX, Zhang YZ, Liu Y (2007) Interaction of loratadine with serum albumins studied by fluorescence quenching method. *J Biochem Biophys Meth* 70: 743–747.